Attenuation correction of PET images with interpolated average CT for thoracic tumors

Abstract

Purpose: To reduce PET and CT misalignments and standard uptake value (SUV) errors, cine average CT (CACT) has been proposed to replace helical CT (HCT) for attenuation correction (AC). A new method using interpolated average CT (IACT) for AC is introduced to further reduce radiation dose with similar image quality.

Materials and Methods: Six patients were recruited in this study. The end-inspiration and expiration phases from a cine CT were used as the two original phases. Deformable image registration was used to generate the interpolated phases. The IACT was calculated by averaging the original and interpolated phases. The PET images were then reconstructed with AC using CACT, HCT and IACT respectively. Their misalignments were compared by visual assessment, mutual information, correlation coefficient and SUV. The doses from different CT maps were analyzed.

Results: The misalignments were reduced for CACT and IACT as compared to HCT. The maximum SUV difference between the use of IACT and CACT was ~3% and it was ~20% between the use of HCT and CACT. The estimated dose for IACT was 0.38 mSv.

Conclusion: The radiation dose using IACT could be reduced by 85% compared to the use of CACT. IACT is a good low-dose approximation of CACT for AC.

Introduction

In modern PET imaging, CT has replaced Ge-68 for the transmission scan. The increased use of CT escalates the risk of radiation exposure for patients (Einstein *et al.*, 2007), and acquisition protocols need to be optimized according to the As Low As Reasonably Achievable (ALARA) philosophy. The drawback of the helical CT (HCT) is the higher radiation dose as compared to Ge-68. Additionally, CT images are usually a snapshot of a respiration cycle, while PET scans are results of average of respiratory cycles. The temporal difference between the scans often introduces misalignment artifacts in PET images.

These misalignments especially introduce misleading tumor locations, volumes and standardized uptake values (SUV) in diagnosing thoracic cancer and radiation treatment planning (Beyer *et al.*, 2004; Charron *et al.*, 2000; Chin *et al.*, 2003; Kinahan *et al.*, 2003; Lardinois *et al.*, 2003; Schöder *et al.*, 2003; Schwaiger *et al.*, 2005; Townsend *et al.*, 2004; Zaidi and Hasegawa, 2003). Reducing the mismatch between HCT and PET in PET/CT via cine average CT (CACT) technique has been proposed (Cook *et al.*, 2007; Dawood *et al.*, 2009; Pan *et al.*, 2005). One concern is that its radiation dose is relatively high.

We previously described the use of the optical flow method (OFM), a deformable image registration algorithm, to register the CT pairs from different time phases and to provide a tissue motion map (Guerrero *et al.*, 2004; Zhang *et al.*, 2008). With this motion map, CT images representing the mid-phases of a respiratory cycle can be obtained by interpolation.

In this study, we develop and evaluate the feasibility of using interpolated average CT (IACT),

generated from the end- expiration and inspiration phases of the cine CT and interpolated phases using deformable image registration, for attenuation correction (AC) purpose. We also assess the potential dose reduction of using IACT.

Materials and methods

PET/CT data acquisition

Six cancer patients were recruited for this study. The tumor locations include left lower lobe, left anterior chest wall, right lower lobe, distal esophagus, right upper lobe, anterior mediastinum and right hilum. Images were acquired on a PET/CT scanner (Discovery VCT, GE Medical Systems, Milwaukee, WI, USA). All patients were injected with 298-458 MBq of ^{18}F-FDG and scanned 1 hour after injection. The default acquisition settings of HCT data were as follows: 120 kV, smart mA (range 40-210 mA) (Kalra *et al*., 2004), i.e. automatic tube current modulation to maintain constant image quality at the lowest dose for different body anatomy, 1.375:1 pitch, 8×2.5 mm x-ray collimation, and 0.5 s CT gantry rotation. Cine CT data were acquired at 120 kV, 10 mA, 8×2.5 mm X-ray collimation, 0.5 s CT gantry rotation and 5.9 s cine CT duration which covers at least one breath cycle. A total of 13 phases in a respiratory cycle from the cine CT were averaged to generate the CACT (Pan *et al.*, 2005). PET data were acquired at 3 min per 15 cm bed position. Our protocol was approved by the local ethics committee and subject number was kept to be minimal, while still showed the significance of the proposed method, to avoid unnecessary radiation exposure. Written informed consents were obtained from all patients.

Deformable image registration

The optical flow method (OFM) (Guerrero *et al.*, 2004; Zhang *et al.*, 2008) was applied to calculate the velocity matrix on two successive CT images in cine CT. The velocity matrix includes

lateral, anterior-posterior and inferior-superior displacements respectively for each voxel. The OFM calculation equation is shown below.

$$v^{(n+1)} = v^{(n)} + \nabla f \left(\frac{\nabla f \cdot v^{(n)} + \frac{\partial f}{\partial t}}{\alpha^2 + \|\nabla f\|^2} \right) \qquad (1)$$

where *n* is the number of iterations and $v^{(n)}$ is the average velocity driven from the surrounding voxels, f is the image intensity, α is the weighting factor of which the value is empirically set at 5 for OFM in CT (Huang *et al*., 2010; Zhang *et al*., 2008).

Interpolated average CT

For IACT calculated from 2 original phases + 11 interpolated phases ($IACT_{2o11i}$), two extreme phases in a cine CT, i.e., normal end-inspiration and expiration, are used to generate the motion maps via OFM. The total motion range for each voxel in the forward motion map is equally spaced into 6 intervals, resulting in 5 sets of interpolated CT images as the mid-phases from inspiration to expiration. Similarly, the backward motion map is used to calculate the 5 mid-phases from expiration to inspiration (Figure 1). The 10 interpolated phases together with the two original phases, plus the next inhalation compose a complete respiratory cycle. These 13 phases are averaged to generate the $IACT_{2o11i}$.

To study the reliability of the proposed IACT technique, different numbers of original phases in the cine CT are used in calculating IACT. Other configurations of the IACTs include 4 original phases + 9 interpolated phases ($IACT_{4o9i}$), 6 original phases + 7 interpolated phases ($IACT_{6o7i}$) and 8 original phases + 5 interpolated phases ($IACT_{8o5i}$).

Image reconstruction

All PET images were reconstructed using OS-EM reconstruction method with 2 iterations and 28 subsets. Attenuation corrections were conducted using the obtained CT maps: HCT, CACT, IACT ($IACT_{2o11i}$, $IACT_{4o9i}$, $IACT_{6o7i}$, $IACT_{8o5i}$), and average CT obtained from 2 extreme phases (ACT). Their reconstructed PET images were compared and their differences of image quality and associated radiation dose were quantified.

Data analysis

Mutual information

In order to provide the overlap invariance, normalized mutual information (MI) was utilized (Studholme *et al.*, 1999). The normalized MI between X and Y, denoted as I(X, Y), is a measure for the statistical dependency between both variables, defined as equation (2). In this study, normalized MI was applied to estimate the non-linear image intensity distribution between IACT/HCT/ACT and CACT.

$$I(X;Y) = \frac{P(X) + P(Y)}{P(X,Y)} \qquad (2)$$

where $P(x)$ is the histogram of X, $P(y)$ is the histogram of Y and $P(x,y)$ is the joint histogram of X and Y. Mutual information represents how much the knowledge of X decreases the uncertainty of Y. Therefore, I(X,Y) is a measure of the shared information between X and Y. The larger the normalized MI values, the more similar two images are (Studholme *et al*., 1999; Zhang *et al*., 2008).

Correlation coefficient

Correlation coefficient (*CC*) was applied to calculate the linear intensity relationship point by point between IACT/HCT/ACT and CACT. The *CC* value represents the total intensity difference

between two image sets, i.e. the summation of the intensity difference for all *n* voxels. The equation defining the *CC* is:

$$CC = \frac{S_{u,v}}{S_u * S_v} = \frac{\sum_{i=1}^{n} \left(u_i - \bar{u}\right) * \left(v_i - \bar{v}\right)}{\sqrt{\sum_{i=1}^{n} \left(u_i - \bar{u}\right)^2} * \sqrt{\sum_{i=1}^{n} \left(v_i - \bar{v}\right)^2}} \qquad (3)$$

where S_u is the standard deviation of object u, S_v is the standard deviation of object v, $S_{u,v}$ is the covariance of object u and v. The value of *CC* is between -1 and 1, indicating negatively correlated to positively correlated respectively.

Both MI and CC methods are capable to give a quantitative measure of similarity between CT images. Since they have different sensitivities to different components of differences, both are included in this study to demonstrate their usage in similarity comparison.

Standardized uptake value (SUV)

PET images reconstructed using HCT, CACT and IACT for AC were compared by visual assessment. The same volumes-of-interest (VOIs) were delineated at the same location around the tumor and the average SUVs in the VOI were obtained. The average SUV values were compared using the following equation:

$$diff_{IACT-CACT} = \frac{\left|SUV_{IACT} - SUV_{CACT}\right|}{SUV_{CACT}} \times 100\% \qquad (4)$$

The differences between the HCT/ACT and CACT techniques, $diff_{HCT\text{-}CACT}$ *and* $diff_{ACT\text{-}CACT}$, were also calculated by replacing IACT with HCT/ACT in the above equation. Smaller values of $diff_{IACT\text{-}CACT}$, $diff_{HCT\text{-}CACT}$ and $diff_{ACT\text{-}CACT}$ indicate better estimations of CACT technique, i.e., less misalignment errors between the associated CT and PET images.

Radiation dose

Radiation dose were expressed by using the volume CT dose index ($CTDI_{vol}$) in Gy, and effective dose in mSv. The dose-length product is defined as the $CTDI_{vol}$ multiplied by scan length, and is an indicator of the integrated radiation dose of an entire CT examination. An approximation of the effective dose was obtained by multiplying the dose-length product by a conversion factor, k (equal to 0.017 $mSv \cdot mGy^{-1} \cdot cm^{-1}$) (ICRP, 2007).

Results

The MI and CC results showed that as the number of original phases in IACT increases, IACT and CACT become more relevant, while $IACT_{2o11i}$ performs better than ACT (Figure 2). Figure 3 shows the sample reconstructed images of HCT, CACT and $IACT_{2o11i}$, their associated PET images and the fused PET/CT images. The only noticeable difference between CACT and $IACT_{2o11i}$ is the higher noise level in $IACT_{2o11i}$ as compared to CACT. This is expected as CACT is an average of all 13 original phases from a cine CT, while $IACT_{2o11i}$ uses only 2 original phases. On the other hand, PET images using HCT for AC demonstrate noticeable artifacts in the diaphragm region. The SUV analysis for HCT, CACT, different IACTs and ACT is shown in Figure 4. For tumors No. 1 through 7, the difference to the one using CACT is smallest when $IACT_{8o5i}$ is used, and it is largest when HCT is used. However, even with $IACT_{2o11i}$ where the difference is the largest among all IACT configurations, it is $\leq$3% as compared to CACT, while the difference was $\geq$10% with maximum difference of ~20%, between the use of HCT and CACT, consistent with the reported values (Pan *et al.*, 2005). The results of ACT are generally inferior to $IACT_{2o11i}$ except for tumor #4.

The effective radiation doses (and $CTDI_{vol}$) from the CT scans are listed in Table 1. The higher dose from HCT, 5.28 mSv (11.18 mGy), is due to the clinical setting of smart mA. In cine CT, the current is set at 10 mA, thus the effective dose is 2.46 mSv (5.17 mGy). If the 2 original phases in the $IACT_{2o11i}$ are replaced by 2 breath-hold CT scans with the same tube current of cine CT, the effective dose would be 0.38 mSv (0.79 mGy), i.e., an 85% reduction from cine CT and a 93% reduction from HCT. In addition, the typical effective dose from ^{18}F-FDG PET imaging is about

10.73 mSv which is invariant with attenuation correction method (Deloar *et al.*, 1998; Wu *et al.*, 2005).

Discussion

The OFM establishes the link between two extreme respiratory phases. With the interpolated phases added, the whole respiratory cycle is constructed. Our results showed that $IACT_{2o11i}$ generally outperforms ACT, demonstrating the effectiveness of this method. The little difference in SUV for PET using IACT and CACT for AC also indicates that IACT is a good approximation of CACT, with the advantage of less radiation dose. For gated PET studies, other approaches for AC are proposed. For example, respiratory gated CT corresponded to the gated PET frames are acquired for phase dependent AC. Other methods include transforming a single CT image to match the associated PET frames through tracking the diaphragm motions in PET (McQuaid *et al.*, 2009). These methods require manual segmentation of the diaphragm and their accuracy highly depends on the motion model.

Motion amplitude may impact the accuracy of the motion maps. Zhong *et al.* (Zhong *et al.*, 2010) showed that the average error in deformable image registration in thoracic regions was around 0.7 mm for a diaphragm motion of 2.6 cm. This accuracy is sufficient for PET AC as PET resolution is much coarser.

The selected lesions located in diversified thoracic regions are representative for general clinical scenarios. Chi *et al.* (Chi *et al.*, 2008) reported that out of 216 lung cancer patients, 68%

had mis-registration and only 10% had an SUV change of > 25% at the tumor location. Four out of seven lesions in our study showed >10% SUV difference between the use of CACT and HCT, with the maximum SUV difference of ~20% for the esophageal lesion which is closest to the diaphragm among all cases.

The drawback of the very low dose setting (10 mA) in both CACT and IACT methods is that the increased noise in the CT images. Noisy attenuation correction data can introduce noise into the PET emission images. As shown in Figure 3B, the emission data for CACT and IACT appear noisier than images corrected with HCT data because of the higher quantum noise in the attenuation correction data in CACT and IACT. If the same signal-to-noise ratio in the emission images of the HCT method is desired, the current setting in CACT and IACT has to be the same as that in the HCT method. The dose to the patient would be higher for the IACT method as compared with HCT, but still much lower than that in CACT. As the purpose of the PET images is to obtain accurate SUV and tumor location and shape, as long as the noise in PET does not affect the extraction of such information, the very low-dose setting should be sufficient for a reasonable attenuation correction CT quality.

It should be noted that the proposed method may not produce better PET image quality as compared with CACT either. The quality of each phase CT in a low-dose 4DCT set is sufficient for clinicians to read. The very low-dose breath-hold CT should possess at least the same quality of each phase CT in the 4DCT as the current and voltage settings are the same, with the residual motion, which often exists in each phase of a 4DCT, not present in the breath-hold CT. The major

advantage of the proposed IACT method is less dose to the patient and yet a good approximation of CACT method in SUV and tumor location.

Clinically, two extreme phases in a cine CT can be replaced by two separate CT scans, one at normal end-inspiration and the other at end-expiration. Since breath-hold CTs are likely different from the phases in free breathing cine CT, an active breath control (ABC) system originally developed by Wong *et al*. for clinical radiotherapy (Wong *et al.*, 1999), can be used to assure breath-hold CTs being taken at desired phases. This non-invasive device integrates a spirometer with a personal computer to control the flow meters and scissor valves. A nose clip is used to ensure that the patients only breathe via the mouthpiece. Patients can be trained using this device prior to the actual CT scanning and CT images can then be taken at desirable lung volume, i.e. particular phase of the breathing cycle. Partridge *et al.* showed that breath-holding time of 15-30 s can be achieved for patients with lung cancer (Partridge *et al.*, 2009). Further study with real breath-hold CT data using ABC is warranted.

Conclusion

The application of IACT for PET AC reduces misalignment artifacts and SUV quantification errors for thoracic tumors as compared to that of HCT. The radiation dose using IACT could be reduced by 85% compared to that of CACT. It serves as a low-dose alternate to CACT. Further study with separate CT scans placed at end-expiration and inspiration phases is needed.

References

Beyer T, Antoch G, Muller S, Egelhof T, Freudenberg L S, Debatin J and Bockisch A 2004 Acquisition protocol considerations for combined PET/CT imaging *J Nucl Med* **45** 25S-35

Charron M, Beyer T, Bohnen N N, Kinahan P E, Dachille M, Jerin J, Nutt R, Meltzer C C, Villemagne V and Townsend D W 2000 Image analysis in patients with cancer studied with a combined PET and CT scanner *Clin. Nucl. Med.* **25** 905-10

Chi P-C M, Mawlawi O, Luo D, Liao Z, Macapinlac H A and Pan T 2008 Effects of respiration-averaged computed tomography on positron emission tomography/computed tomography quantification and its potential impact on gross tumor volume delineation *Int J Radiat Oncol Biol Phys* **71** 890-9

Chin B B, Nakamoto Y, Kraitchman D L, Marshall L and Wahl R 2003 PET-CT evaluation of 2-Deoxy-2-[18F]Fluoro-D-Glucose myocardial uptake: effect of respiratory motion *Molecular Imaging & Biology* **5** 57-64

Cook R A H, Carnes G, Lee T-Y and Wells R G 2007 Respiration-averaged CT for attenuation correction in canine cardiac PET/CT *J Nucl Med* **48** 811-8

Dawood M, Büther F, Stegger L, Jiang X, Schober O, Schäfers M and Schäfers K P 2009 Optimal number of respiratory gates in positron emission tomography: A cardiac patient study *Med Phys* **36** 1775-84

Deloar H M, Fujiwara T, Shidahara M, Nakamura T, Watabe H, Narita Y, Itoh M, Miyake M and Watanuki S 1998 Estimation of absorbed dose for 2-[F-18]fluoro-2-deoxy-glucose using

whole-body positron emission tomography and magnetic resonance imaging *Eur J Nucl Med Mol Imaging* **25** 565-74

Einstein A J, Moser K W, Thompson R C, Cerqueira M D and Henzlova M J 2007 Radiation Dose to Patients From Cardiac Diagnostic Imaging *Circulation* **116** 1290-305

Guerrero T, Zhang G, Huang T-C and Lin K-P 2004 Intrathoracic tumour motion estimation from CT imaging using the 3D optical flow method *Phys Med Biol* **49** 4147-61

Huang T-C, Liang J-A, Dilling T, Wu T-H and Zhang G 2010 Four-dimensional dosimetry validation and study in lung radiotherapy using deformable image registration and Monte Carlo techniques *Radiation Oncology* **5** 45

ICRP 2007 Managing patient dose in multi-detector computed tomography (MDCT) *ICRP Publication 102. Ann. ICRP* **37** 1-80

Kalra M K, Maher M M, Toth T L, Schmidt B, Westerman B L, Morgan H T and Saini S 2004 Techniques and applications of automatic tube current modulation for CT *Radiology* **233** 649-57

Kinahan P E, Hasegawa B H and Beyer T 2003 X-ray-based attenuation correction for positron emission tomography/computed tomography scanners *Semin. Nucl. Med.* **33** 166-79

Lardinois D, Weder W, Hany T F, Kamel E M, Korom S, Seifert B, von Schulthess G K and Steinert H C 2003 Staging of non-small-cell lung cancer with integrated positron-emission tomography and computed tomography *N Engl J Med* **348** 2500-7

McQuaid S J, Lambrou T, Cunningham V J, Bettinardi V, Gilardi M C and Hutton B F 2009 The

application of a statistical shape model to diaphragm tracking in respiratory-gated cardiac PET images *Proceedings of the IEEE* **97** 2039 - 52

Pan T, Mawlawi O, Nehmeh S A, Erdi Y E, Luo D, Liu H H, Castillo R, Mohan R, Liao Z and Macapinlac H A 2005 Attenuation correction of PET images with respiration-averaged CT images in PET/CT *J Nucl Med* **46** 1481-7

Partridge M, Tree A, Brock J, McNair H, Fernandez E, Panakis N and Brada M 2009 Improvement in tumor control probability with active breathing control and dose escalation: A modeling study *Radiother Oncol* **91** 325-9

Schöder H, Erdi Y, Larson S and Yeung H D 2003 PET/CT: a new imaging technology in nuclear medicine *Eur J Nucl Med Mol Imaging* **30** 1419-37

Schwaiger M, Ziegler S and Nekolla S G 2005 PET/CT: challenge for nuclear cardiology *J Nucl Med* **46** 1664-78

Studholme C, Hill D L G and Hawkes D J 1999 An overlap invariant entropy measure of 3D medical image alignment *Pattern Recognition* **32** 71-86

Townsend D W, Carney J P J, Yap J T and Hall N C 2004 PET/CT today and tomorrow *J Nucl Med* **45** 4S-14

Wong J W, Sharpe M B, Jaffray D A, Kini V R, Robertson J M, Stromberg J S and Martinez A A 1999 The use of active breathing control (ABC) to reduce margin for breathing motion *Int J Radiat Oncol Biol Phys* **44** 911-9

Wu T-H, Chu T-C, Huang Y-H, Chen L-K, Mok S-P, Lee J-K, Yeu-Sheng T and Lee J J S 2005 A

positron emission tomography/computed tomography (PET/CT) acquisition protocol for CT radiation dose optimization *Nucl. Med. Commun.* **26** 323-30

Zaidi H and Hasegawa B 2003 Determination of the attenuation map in emission tomography *J Nucl Med* **44** 291-315

Zhang G, Huang T-C, Guerrero T, Lin K-P, Stevens C, Starkschall G and Forster K 2008 Use of three-dimensional (3D) optical flow method in mapping 3D anatomic structure and tumor contours across four-dimensional computed tomography data *J Appl Clin Med Phy* **9** 59-69

Zhong H, Kim J and Chetty I J 2010 Analysis of deformable image registration accuracy using computational modeling *Med Phys* **37** 970-9

Figure legends

Figure 1. The generation of interpolated average CT (IACT). The two extreme phases in a cine CT, end-inspiration and expiration, are registered using optical flow method. The resultant deformation matrix is then used to interpolate the phases in between with equal temporal intervals. The $IACT_{2o11i}$, used for attenuation correction in PET reconstruction, is the average of the two original phases and the interpolated 11 phases.

Figure 2. (A) Values of normalized mutual information (MI) between HCT, ACT, CACT and IACT with different configurations. (B) Values of correlation coefficient (CC) between HCT, ACT, CACT and IACT with different configurations.

Figure 3. (A) Sample reconstructed images of HCT, CACT and $IACT_{2o11i}$, (B) their associated attenuation corrected PET images and (C) PET/CT fused images. Noticeable misalignment artifacts in the diaphragm region (arrow) can be found in the HCT corrected PET.

Figure 4. (A) SUV difference between PET images corrected by HCT, ACT, CACT and IACT with different configurations. (B) Transaxial PET images at the lesion level corrected by (*left*) HCT images, (*middle*) CACT images and (*right*) $IACT_{2o11i}$ images.

Acknowledgements

This study was financially supported in part by the National Science Council of Taiwan (NSC 99-2221-E-039-010) and by the school project of China Medical University, Taiwan (CMU98-C-10). The project was conducted in the campus of NYMU/TVGH.

Author contributions

Guarantors of integrity of entire study: Tung-Hsin Wu；

Study concepts/study design or data acquisition or data analysis/interpretation: Tzung-Chi Huang, Tung-Hsin Wu；

Manuscript drafting or manuscript revision for important intellectual content: Greta S.P. Mok, Geoffrey Zhang；

Approval of final version of submitted manuscript：Tung-Hsin Wu；

Literature research：Tung-Hsin Wu, Greta S.P. Mok, Geoffrey Zhang；

Clinical studies：Shyh-Jen Wang；

Statistical analysis：Tzung-Chi Huang.

keywords: PET, attenuation correction, dose reduction, deformable image registration

Table 1. HCT, CACT and IACT scanning parameters and doses estimation

	HCT	CACT	$IACT_{2\text{-breath hold CT}}$
Scan mode	Helical mode	Axial cine mode	Helical mode
Tube voltage (kVp)	120	120	120
Tube current (mA)	40~210	10	10
Number of phases	1	13	2
$CTDI_{vol}$ (mGy)	11.18	5.17	0.79
Scan coverage (cm)	28	28	28
Dose-length product (mGy ·cm)	310.49	144.62	22.25
Effective dose (mSv)	5.28	2.46	0.38

Figure 1

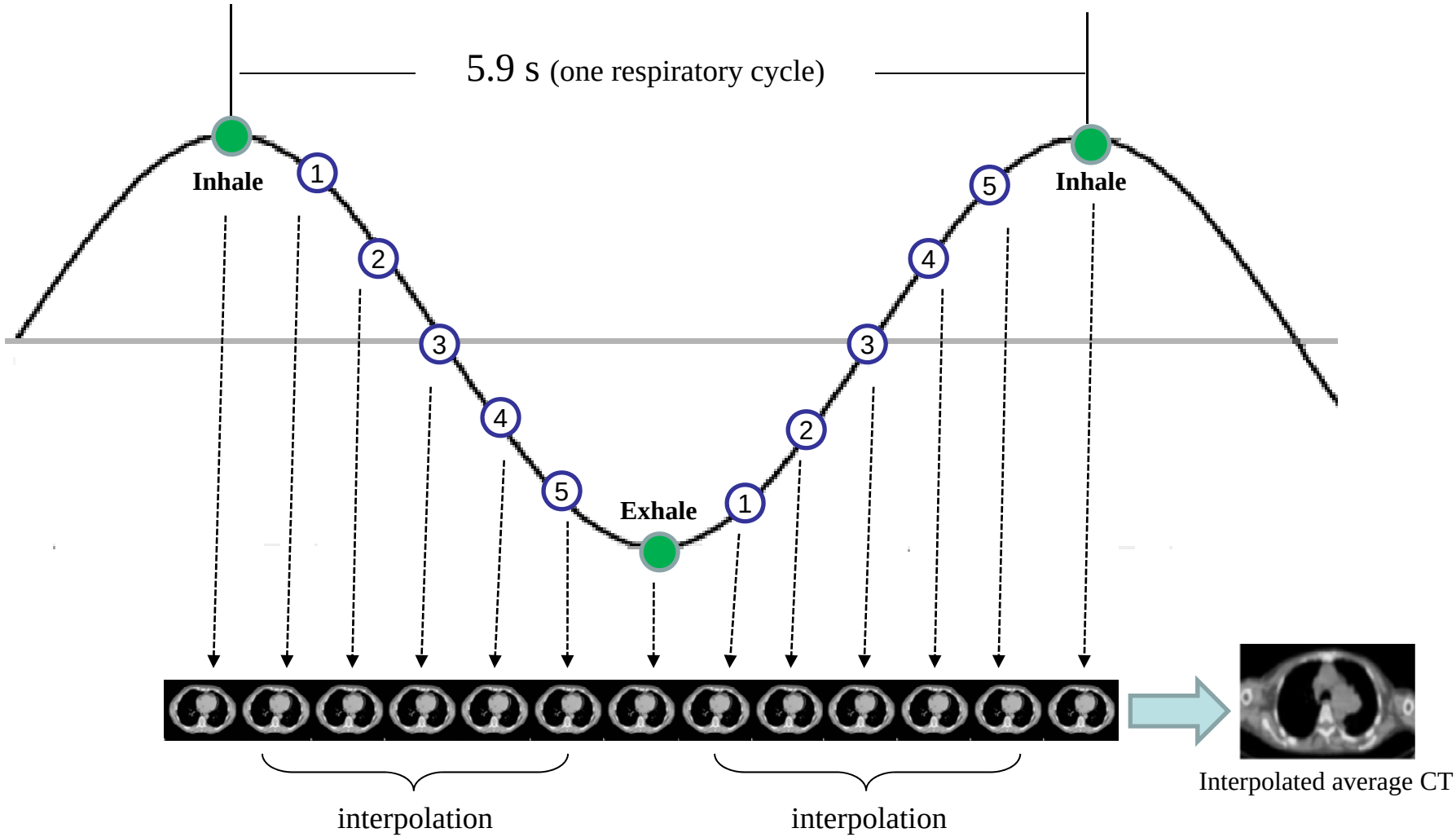
5.9 s (one respiratory cycle)
Inhale
Inhale
Exhale
1
2
3
4
5
1
2
3
4
5
interpolation
interpolation
Interpolated average CT

Figure 2

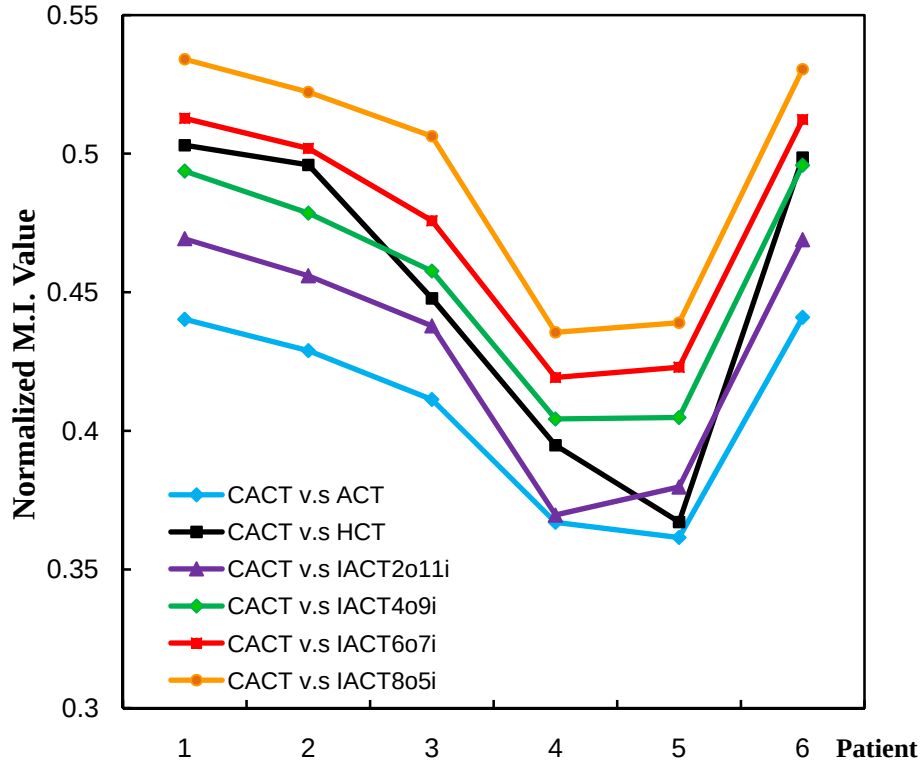
0.55
0.5
0.45
0.4
0.35
0.3
Normalized M.I. Value
CACT v.s ACT
CACT v.s HCT
CACT v.s IACT2o11i
CACT v.s IACT4o9i
CACT v.s IACT6o7i
CACT v.s IACT8o5i
1
2
3
4
5
6
Patient

(A)

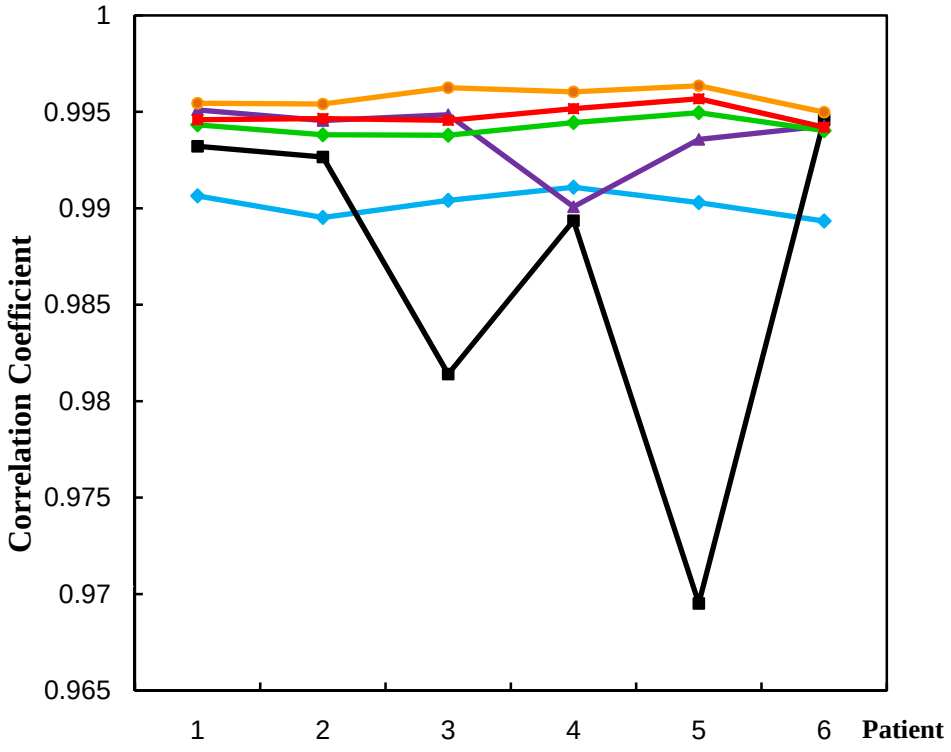
1
0.995
0.99
0.985
0.98
0.975
0.97
0.965
Correlation Coefficient
1
2
3
4
5
6
Patient

(B)

Figure 3

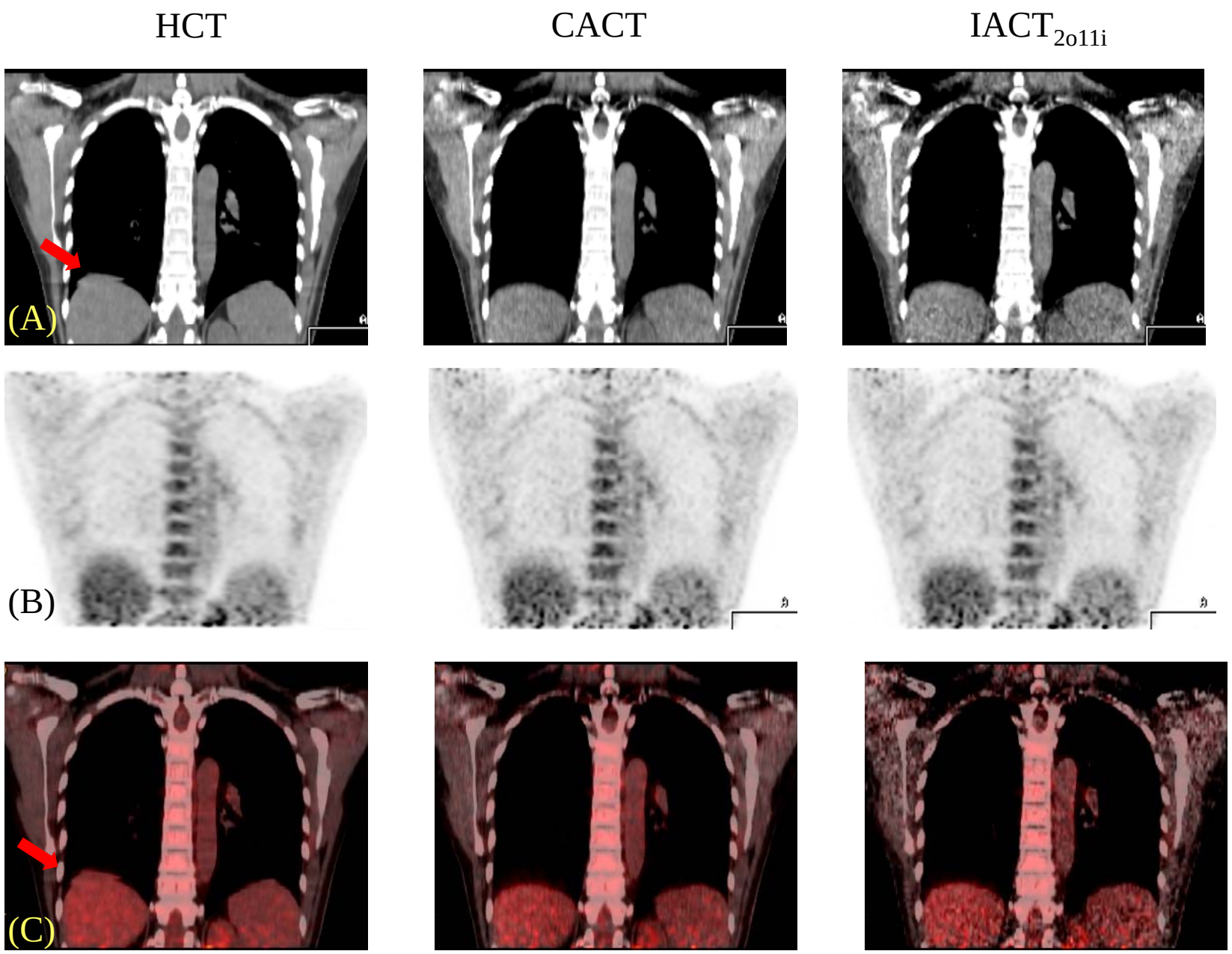

Figure 4

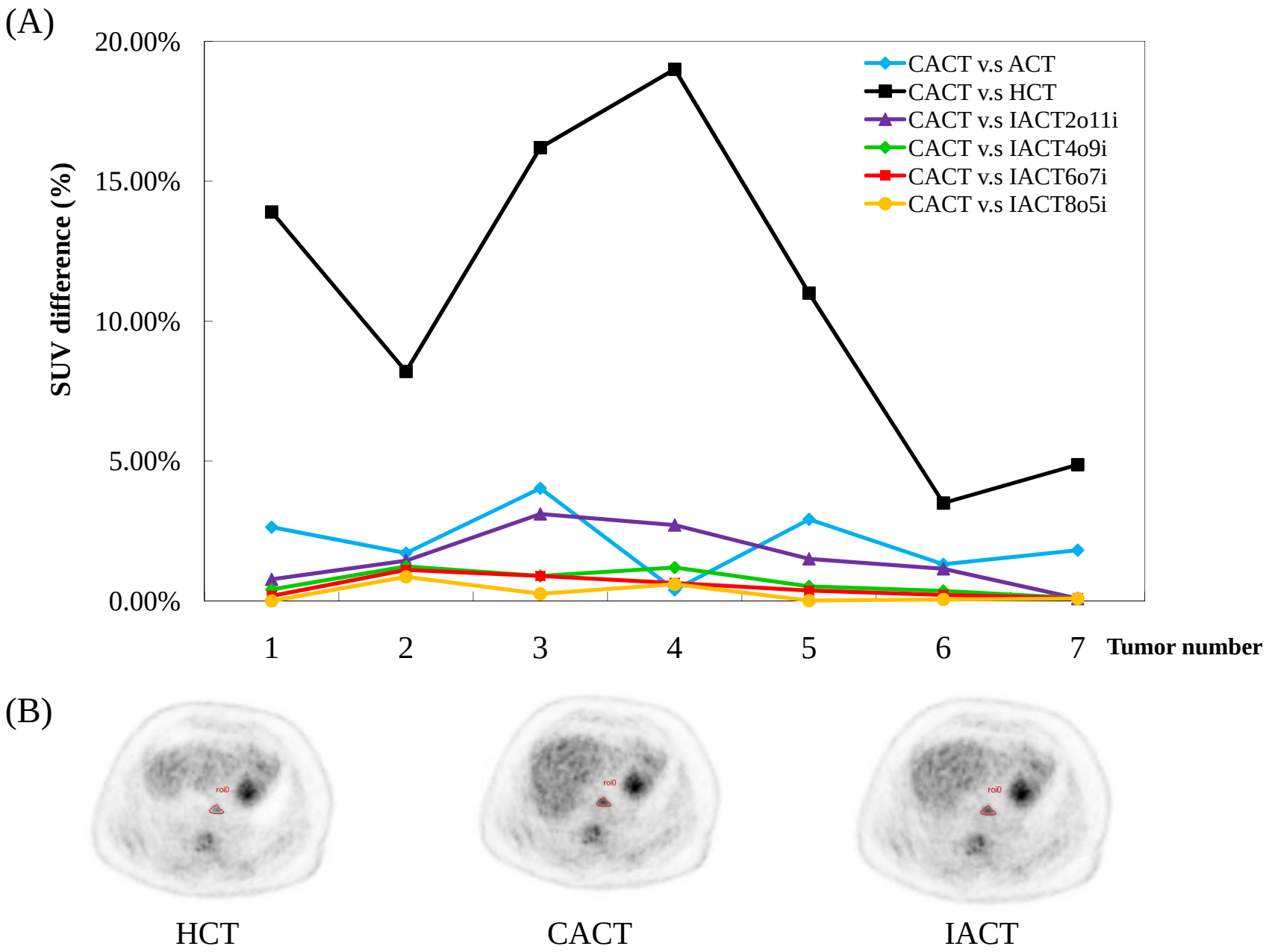
(A)
20.00%
15.00%
10.00%
5.00%
0.00%
SUV difference (%)
CACT v.s ACT
CACT v.s HCT
CACT v.s IACT2o11i
CACT v.s IACT4o9i
CACT v.s IACT6o7i
CACT v.s IACT8o5i
1
2
3
4
5
6
7
Tumor number
(B)
HCT
CACT
IACT